A Comparative Study on the Efficiency of Nickel Oxide/Polyaniline and Cobalt(II,III) Oxide/Polyaniline toward Oxygen Reduction Reaction

Nitish Kumar[1#], Rudra Pratap Udgata[1#], Kajal Tiwari[2], Kingshuk Dutta[3]*, D. Balamurugan[3]

[1]Department of Physics, School of Engineering and Sciences, SRM University, Andhra Pradesh, India, [2]Department of Physics, ICT-Mumbai, Mumbai, Maharashtra, India, [3]Advanced Polymer Design and Development Research Laboratory, School for Advanced Research in Petrochemicals, Central Institute of Petrochemicals Engineering and Technology, Bengaluru, Karnataka, India

[#]These authors contributed equally

ABSTRACT

Polyaniline (PANI) is a conducting polymer that has gained attention as a matrix material for oxygen reduction reaction (ORR) catalysts due to its high surface area, good electrical conductivity, and stability. In this comparative study, the electrochemical properties of nickel oxide (NiO) and cobalt (II,III) oxide (Co_3O_4) catalysts, both embedded in a PANI matrix, were investigated and compared for ORR. The NiO and Co_3O_4 catalysts were synthesized using a simple reduction method and embedded in the PANI matrix through mechanical mixing. The synthesized catalysts were characterized using X-ray diffraction, Fourier-transform infrared spectroscopy, and ultraviolet (UV)-visible spectroscopy. The electrochemical performance of the NiO/PANI and Co_3O_4/PANI catalysts was evaluated using cyclic voltammetry and electrochemical impedance spectroscopy. The results showed that NiO/PANI catalyst possessed slightly higher activity than the Co_3O_4/PANI catalyst. The stability of the catalysts was also investigated from a cyclic voltammogram, where the catalysts were cycled between −0.7 V and 1.5 V for 100 cycles. The results showed that the NiO/PANI and Co_3O_4/PANI catalysts both exhibited good stability. Overall, the comparative study demonstrated that both NiO/PANI and Co_3O_4/PANI catalysts exhibited good electrocatalytic activity and stability for ORR. The study also showed that the PANI matrix provided stable and conductive support for the catalysts. The results suggest that both NiO and Co_3O_4, embedded in a PANI matrix, have the potential to be used as low-cost and efficient catalysts for ORR.

Key words: Oxygen reduction reaction, Electrocatalyst, Nickel oxide, Cobalt oxide, Polyaniline

1. INTRODUCTION

The usage of conventional energy sources such as coal, oil, and gas has led to significant issues including environmental pollution and the greenhouse effect [1,2]. As a result, there has been a lot of interest in the development of sophisticated energy conversion and storage technologies that are affordable, eco-friendly, and non-toxic [3-5]. Direct methanol fuel cells (DMFCs) have certain notable advantages as sustainable and clean energy sources, such as high-energy conversion efficiency, low operating temperature, and little pollutant output [6-9]. Microbial fuel cells (MFCs), a revolutionary electro-biochemical device that can transform organic pollutants into power, have also received a lot of interest. Electrons, produced by organic pollutants that are being broken down by electrogenic bacteria growing on the anode surface, are transmitted to the cathode, where they react with electron acceptors [10,11]. The use of solid oxide fuel cells (SOFC), in which oxygen molecules from the air are reduced to oxygen ions at the cathode and then transferred to the anode to oxidize the fuel molecules, such as H_2 and CO, can accomplish efficient, clean, and direct conversion of chemical energy to electrical energy.

The electrode polarization resistance is thought to be primarily caused by the oxygen reduction process [12]. However, to overcome the significant overpotential of the oxygen reduction reaction (ORR) at the cathodes, effective catalysts are needed. Despite the fact that platinum-based nanoparticles are considered to be the best catalysts for oxygen reduction reactions, non-noble metal catalysts for fuel cell applications have been developed as a result of platinum's rising cost, poor availability, and scarcity [13-15], as well as the ease with which it may be poisoned by a range of compounds (such as HS^-, Cl^-, and CO). Certain transition metals, such as Ni, Co, and Fe, are less expensive, more plentiful, and more toxin-resistant than precious metals, such as Au, Ag, Pt, and Pd [16,17]. As a result, non-precious transition metal alternatives, such as transition metal oxides, hydroxides, and sulfides, as well as their hybrids, have been thoroughly investigated as extremely effective and affordable oxygen catalysts for ORR [18-21].

In recent years, research on catalysts for ORR in fuel cells (namely, DMFC, MFC, PEMFC, and SOFC) has been reported widely. As the ORR at the cathode restricts the overall cell performance, since it is 6 or more orders of magnitude slower than the anode's hydrogen oxidation process; practically, all research and development efforts are directed at developing better cathode catalysts and electrodes. The

following variables are taken into account when considering ORR catalysts for mass production: (a) Lesser generation of H_2O_2 during the ORR and (b) better tolerance of contaminants (such as Cl⁻). Both their durability and cost-effectiveness must be satisfactory. Kinetic losses, mass transport losses, and IR losses are the three processes that reduce the performance of fuel cells. Since kinetic losses are difficult to overcome and increasing the ORR activity would only result in gains of 60 to 70 mV, the ORR predominates in fuel cell kinetic loss [22,23].

The initial publication of cobalt phthalocyanine's ORR activity by Jasinski in 1964 paved the way for a plethora of studies on the synthesis, characterization, and optimization of catalysts consisting of transition metals [24]. Just a few number of studies, to our knowledge, have examined the catalytic activity of transition metals in their oxide or zero-valent states, that is, without the presence of chemically connected heteroatoms. The catalytic activity of nickel electrodes in an alkaline medium toward ORR was studied in the 1960s and 1970s [25]. Such electrodes demonstrated notable oxygen reduction activity when maintained at a lower potential for extended periods of time. Nevertheless, in the absence of this pre-treatment, nickel's strong oxidability caused the development of several surface compounds, which considerably slowed the reaction rate of oxygen reduction. The authors, further, reported in 1976 that hydrogen peroxide was produced by oxygen reduction on NiO through a two-electron mechanism. This was later validated by another group. This work provided a report on the reactivity of nickel and cobalt-based catalysts that are produced using various methods and described the scientific paths used in the attempts to obtain catalysts for ORR [26-28]. Moreover, the disproportionation reaction of hydrogen peroxide, an undesired intermediate in ORR, can be catalyzed by iron group transition metal oxide (i.e., Co_3O_4 and NiO), extending the catalyst lifetime [29,30]. With this backdrop, the present work aimed at comparatively analyzing the efficiency of two of the most promising alternatives to Pt-based catalysts, namely nickel oxide/polyaniline and cobalt(II,III) oxide/polyaniline catalysts, toward oxygen reduction reaction.

2. EXPERIMENTAL

2.1. Materials

Nickel chloride hexahydrate ($NiCl_2.6H_2O$), cobalt(II) nitrate hexahydrate ($Co(NO_3)_2.6H_2O$), sodium borohydride ($NaBH_4$), aniline, ammonium peroxodisulfate (APS), sodium hydroxide (NaOH), HCl (hydrochloric acid), acetone, and methanol were all purchased from Sigma Aldrich were used. De-ionized (DI) water was used for all the experiments.

### 2.2. Synthesis of PANI Support Matrix

In a sample vial, aniline (100 mM) was dissolved in chloroform and allowed to settle. To that solution, 100 mM APS dissolved in 1 M aqueous HCl was added. After 5 min, the polyaniline synthesis at the chloroform water contact is visible. After allowing the reaction to run for 24 h, the fibers were collected by filtration. To remove unreacted monomer and initiator, the polymer nanofibers were thoroughly rinsed with deionized water [31]. A schematic of the catalyst preparation process has been presented in Scheme 1.

2.3. Synthesis of NiO and Co_3O_4

Catalytic precursor salts of nickel chloride hexahydrate ($NiCl_2.6H_2O$) and cobalt(II) nitrate hexahydrate ($Co(NO_3)_2.6H_2O$) were separately combined with deionized water and isopropanol (1:1) to form NiO NPs and Co_3O_4 NPs, respectively, under continuous stirring conditions. For both the salts, the pH of the solutions was raised to 8 after the addition of NaOH. The precursor-ink mixture was then dropwise added 20 mL of 0.2 mol L^{-1} $NaBH_4$ solution for 30 min. The solution was then agitated for 1 h before being cooled and washed with DI water to remove all chloride ions. The catalyst powder was then vacuum-dried at room temperature for 24 h [32-34]. The obtained dried catalysts (80 wt%) were then separately mixed with the PANI support matrix (20 wt%) thoroughly using a mortar pestle for a duration of 30 min.

2.4. Preparation of Working Electrode and Electrochemical Measurements

In a three-electrode system, a glassy carbon electrode was used as the working electrode, a Pt wire as the counter electrode, and Ag/AgCl as the reference electrode. After being sonicated with DI water, the catalyst/support mixture was further mixed with a trace of isopropanol and again ultrasonicated for 30 min to ensure uniform dispersion. The resulting slurry was applied to the surface of the glassy carbon electrode. Before being purged with ultra-pure oxygen gas, all three electrodes were immersed in 0.1 M phosphate buffer solutions. In potential ranges ranging from −0.8 V to +0.8 V, electrochemical cyclic voltammetry (CV) tests were performed. For this purpose, the scanning rate used was 100 mVs^{-1}.
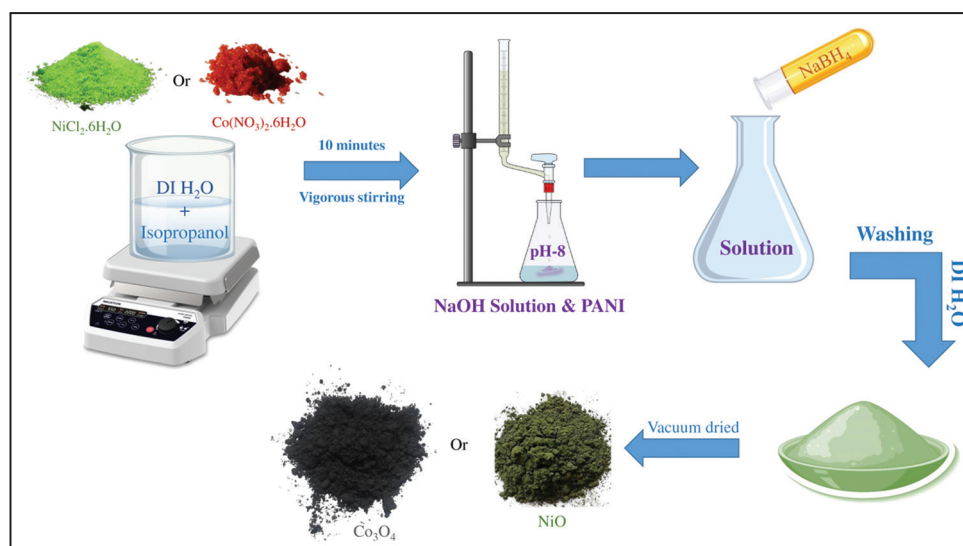
Scheme 1: Steps involved in the synthesis of NiO and Co_3O_4 electrocatalysts embedded in PANI matrix.

2.5. X-Ray Diffractometric (XRD) Analysis

Using a Cu-K$^\alpha$ radiation (1.541 Å) and a fixed scan rate of 1° min^{-1}, XRD patterns of the produced catalyst nanoparticles were recorded by an X-ray diffractometer (Philips Analytical PW1710, Almelo, the Netherlands).

2.6. Electrochemical Impedance Spectroscopic (EIS) Measurements

At 25°C, EIS measurements were taken in a three-electrode cell connected to a computer-aided potentiostat/galvanostat. A catalyst-loaded glassy carbon electrode, a Pt wire, and an Ag/AgCl electrode with oxygen-saturated 0.1 M phosphate buffer solution served as the working, counter, and reference electrodes, respectively. These experiments used a 5 mV amplitude, a frequency range of 30 kHz to 30 mHz, and a potential of 0.3 V. The Nyquist plots were used to evaluate the resistances provided by the cells.

3. RESULTS AND DISCUSSION

3.1. XRD Analysis

The XRD patterns obtained for the Co$_3$O$_4$ and the NiO are shown in Figure 1. The diffraction peaks obtained for the Co$_3$O$_4$ at 2θ values of 31.19°, 36.65°, 44.62°, 55.52°, 59.19°, and 65.1° represent the (220), (311), (400), (422), (511), and (440) planes of Co$_3$O$_4$, respectively [35]. Further, the strong diffraction peaks obtained for the NiO at 2θ values of 36.84°, 43.20°, 62.53°, 74.99°, and 78.72° correspond to the (111), (200), (220), (311), and (222) facets, respectively [36]. There were no impurity peaks observed for nickel oxide. Figure 1 further presents the XRD patterns obtained for PANI, NiO/PANI, and Co$_3$O$_4$/PANI at room temperature. The diffraction peaks obtained at 2θ values 15.1°, 20.7°, and 25.5° represent (011), (020), and (200) planes of PANI, respectively [37].

3.2. FT-IR Analysis

Figure 2b and c show the Fourier-transform infrared spectroscopy spectra obtained for NiO and Co$_3$O$_4$. Co$_3$O$_4$ showed three absorption bands at 3738, 1741, and 1516 cm^{-1}, which belong to absorbed water molecules. Moreover, there are two particular bonds produced from the stretching vibration of the Co-oxide bond. The first one is at 663 cm^{-1}, resulting from the vibration of Co(III)-O bonds, and the second one is at 567 cm^{-1}, related to the Co-stretching [38]. In NiO, peaks at 746.45 and 860.2 cm^{-1} were observed because of Ni-O bond stretching vibration [39]. The broadness of the peak indicated that the

synthesized NiO is crystalline in nature. The broad peaks observed at 3450.6, 1645, and 1427 cm^{-1} may be due to the stretching and bending vibrations of –OH group absorbed on the catalyst surface from the atmosphere. The characteristic peaks of PANI [Figure 2a] were also clearly realized, with some extent of shifting, in the spectra of Nio/PANI and Co$_3$O$_4$/PANI mixtures [Figure 2b and c].

3.3. UV Analysis

Figure 3 depicts the UV-visible absorption spectra of NiO and Co$_3$O$_4$ nanoparticles obtained at room temperature. The value of the absorption of NiO particles was 385 nm, while for Co$_3$O$_4$ particles, it was 270 nm [40,41]. These peaks correspond to the formation of NiO and Co$_3$O$_4$ particles. The optical band gaps of NiO and Co$_3$O$_4$ particles have been calculated from the corresponding absorption spectrum using the energy wavelength relation, as given by Eq. (1).

$$Eg = h\nu/\lambda \tag{1}$$

Where E stands for Energy and λ for wavelength. The corresponding band gap energies of NiO and Co$_3$O$_4$ have been calculated as 3.2 eV for NiO and 4.5 eV for Co$_3$O$_4$.

3.4. Electrochemical Characterizations

CV analysis was performed using a three-electrode system with a glassy carbon working electrode, a platinum wire counter electrode, and an Ag/AgCl reference electrode to determine the ORR catalyst activities of the prepared electrocatalysts. On the working electrode surface, NiO/PANI and Co$_3$O$_4$/PANI samples were deposited. CV measurements were taken in an oxygen-saturated 0.1 M phosphate buffer solution at scan rates of 50, 100, 150, and 200 mVs^{-1}. It was observed that for both NiO/PANI [Figure 4b] and Co$_3$O$_4$/PANI [Figure 4a], the CV curves had well-defined redox peaks, indicating the presence of reversible redox reactions. The cathodic and anodic peaks were found at potentials ranging from -0.7 V to 1.5 V versus Ag/AgCl, which is typical for ORR catalysis. The peak currents observed for NiO and Co$_3$O$_4$ were 0.65 and 0.38 mAcm^{-2}, respectively, indicating that NiO/PANI has slightly greater electrocatalytic activity for ORR than Co$_3$O$_4$/PANI.

Figure 4c shows that the forward peak potential (E$_F$) of the synthesized NiO/PANI shifted more positively (100 mV) than that of the synthesized Co$_3$O$_4$/PANI. At a potential of 0.0 V, the prepared NiO/PANI exhibited a backward peak potential (E$_B$), that is, the cathodic peak. When the NiO/PANI was used for the ORR, a 100 mV shift was obtained when compared to the Co$_3$O$_4$/PANI. The onset potential and half-wave potential of NiO/PANI and Co$_3$O$_4$/PANI for ORR were determined from the CV curves to further investigate their electrocatalytic activity. For both NiO/PANI and Co$_3$O$_4$/PANI, the onset potential (or the potential at which the current begins to increase) was found to be 1 V versus Ag/AgCl. The half-wave potential for NiO/PANI was found to be 0.5 V versus Ag/AgCl and 0.55 V versus Ag/AgCl for Co$_3$O$_4$/PANI.

The stability of NiO and Co$_3$O$_4$ for ORR can be assessed from Figure 4d, which was obtained by performing CV measurements after 100 cycles. The CV curves for NiO and Co$_3$O$_4$ both showed small significant changes in the peak positions or shapes, indicating that the materials are less stable over repeated ORR cycles.

3.5. Electrochemical Impedance Spectroscopic Analysis

Impedance data were analyzed by fitting it to the equivalent circuit, as shown in Figure 5 (inset). In this circuit, R$_s$, CPE, and R$_{ct}$ represent the solution resistance, a constant phase element corresponding to the double-layer capacitance and the charge transfer resistance associated with the ORR, respectively. Nyquist plots have been obtained for the NiO/PANI and the Co$_3$O$_4$/PANI in O$_2$-saturated 0.1 M phosphate buffer solutions at room temperature [Figure 5]. The resultant impedance
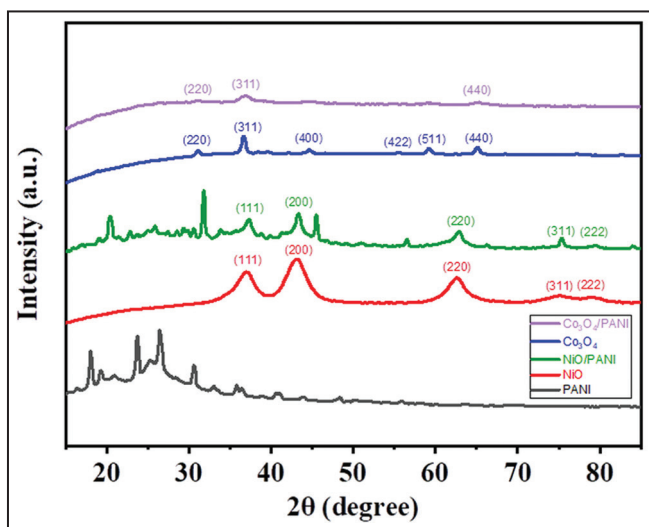

Figure 1: X-ray diffraction spectra of PANI, NiO, Co$_3$O$_4$, NiO/PANI, and Co$_3$O$_4$/PANI.
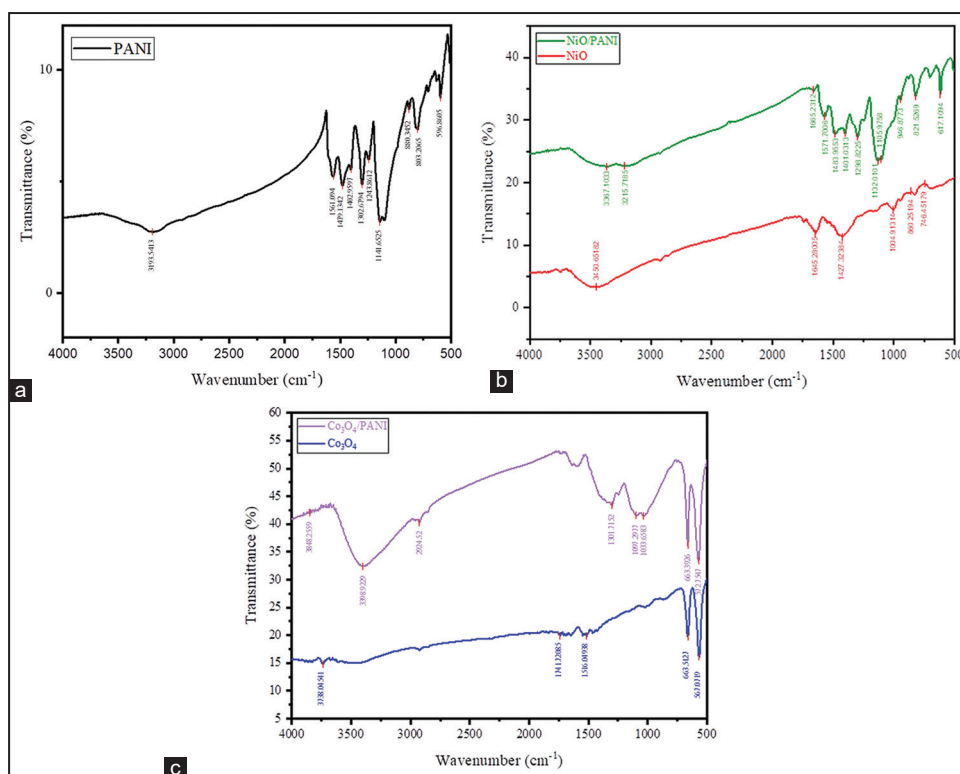
Figure 2: Fourier-transform infrared spectroscopy spectra of (a) PANI, (b) NiO and NiO/PANI, and (c) Co_3O_4 and Co_3O_4/PANI.
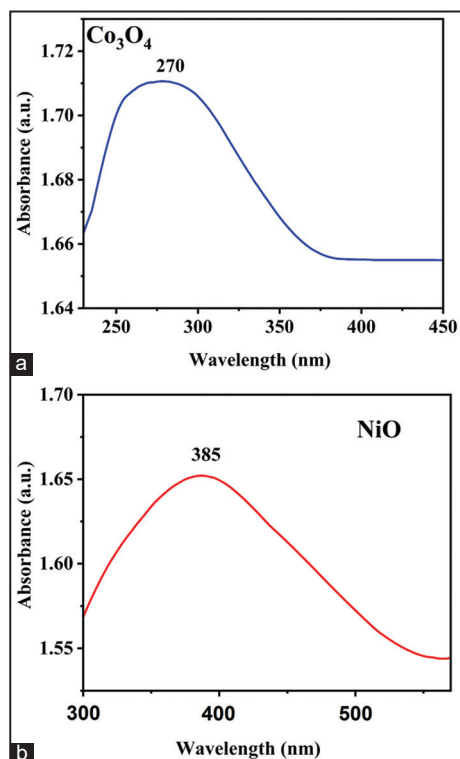

Figure 3: Ultraviolet-visible spectra of (a) Co_3O_4 and (b) NiO.

value obtained for the NiO/PANI was lower than that obtained for the Co_3O_4/PANI catalyst. This result suggests that the conductivity of the synthesized NiO/PANI is comparatively higher than Co_3O_4/PANI catalyst. The Co_3O_4/PANI exhibited a higher R_{ct} value of 30 Ω than that obtained for NiO/PANI, that is, 18 Ω, which was responsible for the deactivation of the reaction kinetics.

3.6. Cost Analysis

The ORR is a critical reaction in many energy conversion devices, including fuel cells and metal-air batteries. Pt is widely used as the catalyst for ORR due to its high activity, but it is expensive and rare [42]. Therefore, researchers have been investigating alternative catalysts that are more abundant and less expensive, such as the ones presented in this work – NiO and Co_3O_4. Cost analysis of NiO and Co_3O_4 compared to Pt for ORR depends on several factors, including the cost of the raw materials, the cost of processing the materials, and the performance of the catalysts. In terms of the cost of raw materials, NiO and Co_3O_4 are significantly cheaper than Pt. According to the periodic table of elements, the cost of nickel and cobalt is around 3–4 orders of magnitude cheaper than platinum. However, NiO and Co_3O_4 have lower electrocatalytic activity compared to Pt and, therefore, require larger amount of catalyst to achieve the same performance [43]. Therefore, the overall cost of using NiO and Co_3O_4 can be comparable or higher than Pt, depending on the specific application and performance requirements. Furthermore, the stability and durability of NiO and Co_3O_4 are inferior to Pt, which may require more frequent replacements, leading to a higher long-term cost [44]. Nonetheless, recent advances in material synthesis and catalyst design have shown improvements in the activity and stability of NiO and Co_3O_4, making them a promising alternative to Pt.

The overall expense involved in the synthesis of the catalyst, taking into account the cost of the chemicals used and the energy consumption during the entire process (i.e., reduction, ultra-sonication, stirring, filtration, cooling, washing, and drying) for NiO, Co_3O_4, and PANI was in the range of US $25 to $35/g. On the other hand, the cost of the commercial Pt-NPs (Sigma Aldrich [St Louis, MO, USA], CAS Number 7440-06-4) was US $197 per gram. Therefore, a considerable reduction in the cathode catalyst's cost can be realized on using NiO and Co_3O_4 in place of the commercially available Pt-NPs.
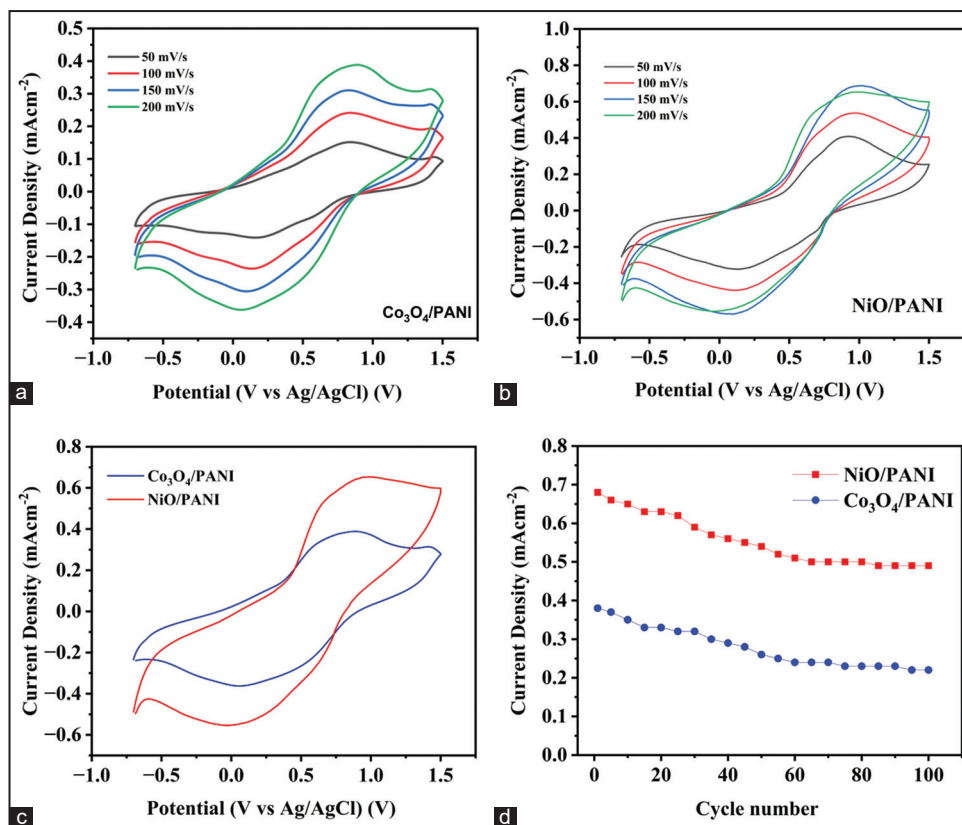
Figure 4: Cyclic voltammetry representing (a) CV curves of Co_3O_4/PANI at different scan rates, (b) CV curves of NiO/PANI at different scan rates, (c) CV curves of Co_3O_4/PANI and NiO/PANI at a scan rate of 200 mVs^{-1}, and (d) cyclic stability for 100 cycles in O_2 saturated 0.1 M phosphate buffer solution at a scan rate of 200 mVs^{-1}.
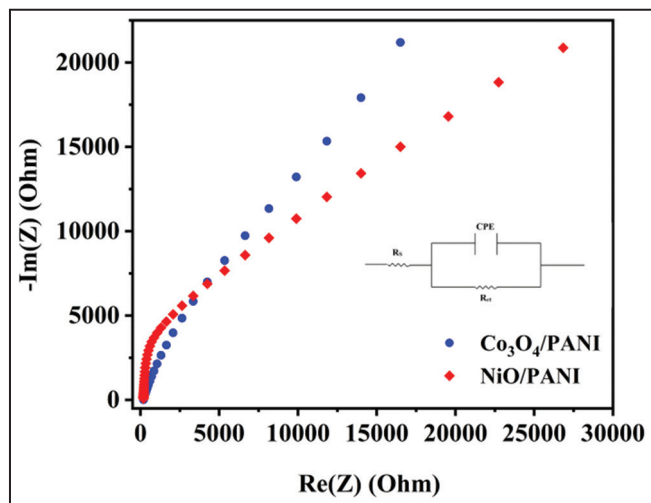

Figure 5: Nyquist plots obtained for Co_3O_4/PANI and NiO/PANI at −0.3 V (vs. Ag/AgCl) at room temperature, and the corresponding equivalent circuit (inset).

4. CONCLUSION

The synthesized cathode electrocatalysts, NiO/PANI and Co_3O_4/PANI, for oxygen reduction reaction (ORR) have shown promising results. These catalysts have demonstrated good catalytic activity for ORR, and their performance can be further enhanced by optimizing their composition, morphology, and surface structure. NiO catalysts have shown to be more stable and durable than Co_3O_4 catalysts under ORR conditions. The addition of other metals or doping elements can significantly improve the ORR activity and stability of NiO and Co_3O_4 catalysts. The NiO and Co_3O_4 with polyaniline, functioning both as a support matrix and a binding agent, have shown promising results as a Nafion-free catalyst, exhibiting excellent electrochemical performance, with high activity, stability, and durability, comparable to or even better than traditional Nafion-based catalysts. These results indicate that NiO and Co_3O_4 with polyaniline have great potential for use in fuel cell and other energy conversion devices, and can pave the way for the development of new and more efficient Nafion-free catalysts for ORR.

5. DECLARATIONS

5.1. Ethical Approval

Not applicable.

6. COMPETING INTERESTS

The authors declare no competing interests.

7. AUTHORS' CONTRIBUTIONS

N.K., R.P.U., K.T., and D.B. performed the experiments, K.D. conceptualized the research idea, N.K., R.P.U., and K.D. wrote the main manuscript text, N.K., and R.P.U. prepared the figures, and K.D. provided the research guidance. All authors reviewed the manuscript.

8. FUNDING

9. AVAILABILITY OF DATA AND MATERIALS

The data that support the findings of this study are available from the corresponding author on reasonable request.

10. REFERENCES

1. H. Pan, Y. Cao, B. Zhang, J. Han, Y. Bai, X. Shang, Z. Jiang, X. Tian, Z. J. Jiang, (2021) Amino functionalized carbon nanotubes supported CoNi@CoO-NiO core/shell nanoparticles as highly efficient bifunctional catalyst for rechargeable Zn-air batteries, *International Journal of Hydrogen Energy*, **46:** 374-388.

2. J. Zhang, X. Bai, T. Wang, W. Xiao, P. Xi, J. Wang, D. Gao, J. Wang, (2019) Bimetallic nickel cobalt sulfide as efficient electrocatalyst for Zn-air battery and water splitting, *Nano-Micro Letters*, **11:** 2.

3. P. Li, B. Wei, Z. Lü, Y. Wu, Y. Zhang, X. Huang, (2019) La$_{1.7}$Sr$_{0.3}$Co$_{0.5}$Ni$_{0.5}$O$_{4+}$$^{\delta}$ layered perovskite as an efficient bifunctional electrocatalyst for rechargeable Zinc-air batteries, *Applied Surface Science*, **464:** 494-501.

4. J. Deng, L. Yu, D. Deng, X. Chen, F. Yang, X. Bao, (2013) Highly active reduction of oxygen on a feco alloy catalyst encapsulated in pod-like carbon nanotubes with fewer walls, *Journal of Materials Chemistry A*, **1:** 14868-14873.

5. S. Li, W. Chen, H. Pan, Y. Cao, Z. Jiang, X. Tian, X. Hao, T. Maiyalagan, Z. J. Jiang, (2019) FeCo alloy nanoparticles coated by an ultrathin N-doped carbon layer and encapsulated in carbon nanotubes as a highly efficient bifunctional air electrode for rechargeable Zn-air batteries, *ACS Sustainable Chemistry and Engineering*, **7:** 8530-8541.

6. C. D. Gu, M. L. Huang, X. Ge, H. Zheng, X. L. Wang, J. P. Tu, (2014) NiO electrode for methanol electro-oxidation: Mesoporous vs. Nanoparticulate, l*nternational Journal of Hydrogen Energy*, **39:** 10892-10901.

7. F. Hong, M. Wang, Y. Ni, (2018) NiO-CoO hybrid nanostructures: Preparation, characterization and application in methanol electro-oxidation, *Journal of Cluster Science*, **29:** 663-672.

8. Y. Y. Tong, C. D. Gu, J. L. Zhang, M. L. Huang, H. Tang, X.L. Wang, J. P. Tu, (2015) Three-dimensional astrocyte-network Ni-P-O compound with superior electrocatalytic activity and stability for methanol oxidation in alkaline environments, *Journal of Materials Chemistry A*, **3:** 4669-4678.

9. M. Jafarian, M. G. Mahjani, H. Heli, F. Gobal, H. Khajehsharifi, M. H. Hamedi, (2003) A study of the electro-catalytic oxidation of methanol on a cobalt hydroxide modified glassy carbon electrode, *Electrochimica Acta*, **48:** 3423-3429.

10. B. Li, X. Zhou, X. Wang, B. Liu, B. Li, (2014) Hybrid binuclear-cobalt-phthalocyanine as oxygen reduction reaction catalyst in single chamber microbial fuel cells, *Journal of Power Sources*, **272:** 320-327.

11. M. Zhou, M. Chi, J. Luo, H. He, T. Jin, (2011) An overview of electrode materials in microbial fuel cells, *Journal of Power Sources*, **196:** 4427-4435.

12. M. Nadeem, B. Hu, C. Xia, (2018) Effect of NiO addition on oxygen reduction reaction at lanthanum strontium cobalt ferrite cathode for solid oxide fuel cell, *International Journal of Hydrogen Energy*, **43:** 8079-8087.

13. T. Y. Yung, L. Y. Huang, T. Y. Chan, K. S. Wang, T. Y. Liu, P. T. Chen, C. Y. Chao, L. K. Liu, (2014) Synthesis and characterizations of Ni-NiO nanoparticles on pdda-modified graphene for oxygen reduction reaction, *Nanoscale Research Letters*, **9:** 444.

14. H. Ataee-Esfahani, M. Imura, Y. Yamauchi, (2013) All-metal mesoporous nanocolloids: Solution-phase synthesis of core-shell Pd@Pt nanoparticles with a designed concave surface, *Angewandte Chemie International Edition*, **52:** 13611-13615.

15. M. K. Debe, (2012) Electrocatalyst approaches and challenges for automotive fuel cells, *Nature*, **486:** 43-51.

16. Y. Yang, X. Sun, G. Han, X. Liu, X. Zhang, Y. Sun, M. Zhang, Z. Cao, Y. Sun, (2019) Enhanced electrocatalytic hydrogen oxidation on Ni/NiO/C derived from a nickel-based metal-organic framework, *Angewandte Chemie International Edition*, **58:** 10644-10649.

17. J. Shen, Y. Hu, C. Li, C. Qin, M. Ye, (2008) Pt-Co Supported on single-walled carbon nanotubes as an anode catalyst for direct methanol fuel cells, *Electrochimica Acta*, **53:** 7276-7280.

18. T. Wang, G. Nam, Y. Jin, X. Wang, P. Ren, M. G. Kim, J. Liang, X. Wen, H. Jang, J. Han, Y. Huang, Q. Li, J. Cho, (2018) NiFe (Oxy) hydroxides derived from NiFe disulfides as an efficient oxygen evolution catalyst for rechargeable Zn-air batteries: The effect of surface S residues, *Advanced Materials*, **30:** 1800757.

19. Y. Xiao, P. Zhang, X. Zhang, X. Dai, Y. Ma, Y. Wang, Y. Jiang, M. Liu, Y. Wang, (2017) Bimetallic thin film NiCo-NiCoO$_2$@NC as a superior bifunctional electrocatalyst for overall water splitting in alkaline media, *Journal of Materials Chemistry A*, **5:** 15901-15912.

20. C. Yu, J. Lu, L. Luo, F. Xu, P. K. Shen, P. Tsiakaras, S. Yin, (2019) Bifunctional catalysts for overall water splitting: CoNi oxyhydroxide nanosheets electrodeposited on titanium sheets, *Electrochimica Acta*, **301:** 449-457.

21. Z. Yang, X. Liang, (2020) Self-magnetic-attracted Ni$_x$Fe$_{(1-x)}$@Ni$_x$Fe$_{(1-x)}$O nanoparticles on nickel foam as highly active and stable electrocatalysts towards alkaline oxygen evolution reaction, *Nano Research*, **13:** 461-466.

22. C. Li, Y. Yamauchi, (2013) Facile solution synthesis of Ag@Pt core-shell nanoparticles with dendritic Pt shells, *Physical Chemistry Chemical Physics*, **15:** 3490-3496.

23. J. Ahmed, Y. Yuan, L. Zhou, S. Kim, (2012) Carbon supported cobalt oxide nanoparticles-iron phthalocyanine as alternative cathode catalyst for oxygen reduction in microbial fuel cells, *Journal of Power Sources*, **208,** 170-175.

24. R. Jasinski, (1964) A new fuel cell cathode catalyst, *Nature*, **201:** 1212-1213.

25. V. S. Bagotzky, N. A. Shumilova, E. I. Khrushcheva, (1976) Electrochemical oxygen reduction on oxide catalysts, *Electrochimica Acta*, **21:** 919-924.

26. S. N. S. Goubert-Renaudin, A. Wieckowski, (2011) Ni and/or Co nanoparticles as catalysts for Oxygen Reduction Reaction (ORR) at room temperature, *Journal of Electroanalytical Chemistry*, **652:** 44-51.

27. C. C. Chang, T. C. Wen, (1997) An investigation of thermally prepared electrodes for oxygen reduction in alkaline solution, *Materials Chemistry and Physics*, **47:** 203-210.

28. M. Hamdani, R. N. Singh, P. Chartier, (2010) Co$_3$O$_4$ and co-based spinel oxides bifunctional oxygen electrodes, *International Journal of Electrochemical Science*, **5:** 556-577.

29. V. B. Oliveira, M. Simões, L. F. Melo, A. M. F. R. Pinto, (2013) Overview on the developments of microbial fuel cells, *Biochemical Engineering Journal*, **73:** 53-64.

30. F. Zhao, R. C. Slade, J. R. Varcoe, (2009) Techniques for the study and development of microbial fuel cells: An electrochemical perspective, *Chemical Society Reviews*, **38:** 1926-1939.

31. K. Dutta, R. Y. Mahale, A. Arulkashmir, K. Krishnamoorthy, (2012) Reversible assembly and disassembly of micelles by a

polymer that switches between hydrophilic and hydrophobic wettings, *Langmuir*, **28:** 10097-10104.

32. S. Das, K. Dutta, P. P. Kundu, (2015) Nickel nanocatalysts supported on sulfonated polyaniline: Potential toward methanol oxidation and as anode materials for DMFCs, *Journal of Materials Chemistry A*, **3:** 11349-11357.

33. D. Xu, P. Dai, X. Liu, C. Cao, Q. Guo, (2008) Carbon-supported cobalt catalyst for hydrogen generation from alkaline sodium borohydride solution, *Journal of Power Sources*, **182:** 616-620.

34. S. Das, K. Dutta, P. P. Kundu, (2016) Sulfonated polypyrrole matrix induced enhanced efficiency of Ni nanocatalyst for application as an anode material for DMFCs, *Materials Chemistry and Physics*, **176:** 143-151.

35. P. Dutta, M. S. Seehra, S. Thota, J. Kumar, (2008) A comparative study of the magnetic properties of bulk and nanocrystalline Co_3O_4, *Journal of Physics: Condensed Matter*, **20:** 015218.

36. Z. Wei, H. Qiao, H. Yang, C. Zhang, X. Yan, (2009) Characterization of NiO nanoparticles by anodic arc plasma method, *Journal of Alloys and Compounds*, **479:** 855-858.

37. Y. Zhang, J. Liu, Y. Zhang, J. Liu, Y. Duan, (2017) Facile synthesis of hierarchical nanocomposites of aligned polyaniline nanorods on reduced graphene oxide nanosheets for microwave absorbing materials, *RSC Advances*, **7:** 54031-54038.

38. X. Hongyan, Z. Hai, J. Diwu, Q. Zhang, L. Gao, D. Cui, J. Zang, J. Liu, C. Xue, (2015) Synthesis and microwave absorption properties of core-shell structured Co_3O_4-PANI nanocomposites, *Journal of Nanomaterials*, **2015:** 1-8.

39. Z. N. Kayani, M. Z. Butt, S. Riaz, S. Naseem, (2018) Synthesis of NiO nanoparticles by sol-gel technique, *Materials Science-Poland*, **36:** 547-552.

40. N. O. M. Dewi, Y. Yulizar, D. O. B. Apriandanu, (2019) Green synthesis of Co_3O_4 nanoparticles using euphorbia heterophylla L. Leaves extract: Characterization and photocatalytic activity, *IOP Conference Series Materials Science and Engineering*, **509:** 012105.

41. J. Adhikary, P. Chakraborty, B. Das, A. Datta, S. K. Dash, S. Roy, J. W. Chen, T. Chattopadhyay, (2015) Preparation and characterization of ferromagnetic nickel oxide nanoparticles from three different precursors: Application in drug delivery, *RSC Advances*, **5:** 35917-35928.

42. X. Tian, X. F. Lu, B. Y. Xia, X. W. Lou, (2020) Advanced electrocatalysts for the oxygen reduction reaction in energy conversion technologies, *Joule*, **4:** 45-68.

43. G. Yanalak, A. Aljabour, E. Aslan, F. Ozel, I. H. Patir, M. Kus, M. Ersoz, (2018) NiO and Co_3O_4 nanofiber catalysts for the hydrogen evolution reaction at liquid/liquid interfaces, *Electrochimica Acta*, **291:** 311-318.

44. S. Das, K. Dutta, A. Enotiadis, F. Papiya, P. P. Kundu, S. K. Bhattacharya, E. P. Giannelis, (2020) Nanorods of cerium oxide as an improved electrocatalyst for enhanced oxygen reduction in single-chambered microbial biofuel cells, *Materials Research Express*, **7:** 015514.

*Bibliographical Sketch

Dr. Kingshuk Dutta is currently employed as a Scientist at CIPET, India. Prior to this appointment, he had worked as an Indo-U.S. Postdoctoral Fellow at Cornell University and as a National Postdoctoral Fellow at IIT – Kharagpur, both funded by DST-SERB. Earlier, as a Senior Research Fellow funded by CSIR, he had carried out his doctoral study at University of Calcutta. He has been a recipient of the prestigious GATE and National Scholarship, both from MHRD; and was also awarded the Dr. D. S. Kothari Postdoctoral Fellowship by UGC. His areas of research interest lie in the fields of electrochemical devices and water treatment. Until date, he has contributed to 66 articles in reputed international platforms, 30 book chapters and many national and international presentations. In addition, he has edited/co-edited 7 books published by Elsevier, the American Chemical Society and Wiley. He is a life member and an elected fellow of the Indian Chemical Society, the International Society for Development & Sustainability, and the Scholars Academic & Scientific Society. He is also the recipient of the Vivekananda Prize from Institute of Researchers.